International Conference on Adaptive Modeling and Simulation
ADMOS 2021
F. Larsson and P. Díez

AN ADAPTIVE METHOD FOR THE NUMERICAL SOLUTION OF A 2D MONGE-AMPÈRE EQUATION

A. CABOUSSAT*, D. GOURZOULIDIS† AND M. PICASSO‡

* Geneva School of Business Administration, University of Applied Sciences and Arts Western Switzerland (HES-SO), alexandre.caboussat@hesge.ch, http://campus.hesge.ch/caboussat

† Geneva School of Business Administration, University of Applied Sciences and Arts Western Switzerland (HES-SO), and Institute of Mathematics, Ecole polytechnique fédérale de Lausanne, 1015 Lausanne, Switzerland, dimitrios.gourzoulidis@hesge.ch, dimitrios.gourzoulidis@epfl.ch

‡ Institute of Mathematics, Ecole polytechnique fédérale de Lausanne, 1015 Lausanne, Switzerland, marco.picasso@epfl.ch

Key words: Monge-Ampère equation, Adaptive mesh refinement, Time-stepping algorithm, Non-smooth solutions

Abstract. An adaptive mesh refinement method for the solution of the elliptic Monge-Ampère equation in two dimensions of space is presented. The solution of the elliptic Monge-Ampère equation is obtained through a numerical method based on a time-stepping strategy for the corresponding flow problem. Continuous piecewise linear finite elements are used for the space discretization. The error is bounded above by an error indicator plus an extra term that can be disregarded in special cases. Numerical experiments exhibit appropriate convergence orders and a robust behavior. Adaptive mesh refinement proves to be efficient and accurate to tackle test cases with singularities.

1 THE MONGE-AMPÈRE EQUATION

Let Ω be a smooth bounded convex domain of $\mathbb{R}^2$. We consider the elliptic two-dimensional Monge-Ampère equation, with Dirichlet boundary conditions, which reads as follows: find $u : \Omega \to \mathbb{R}$ satisfying

$$\begin{cases} \det \mathbf{D}^2 u = f & \text{in } \Omega, \\ u = g & \text{on } \partial\Omega, \end{cases} \tag{1}$$

Here $f > 0$, g are given functions with the required regularity, and $\mathbf{D}^2 u$ is the Hessian of the unknown function u. In order to accurately approximate the solution of (1), we

consider the corresponding flow problem and look for a stationary solution of the time-evolutive problem: find $u : \Omega \times (0,T) \to \mathbb{R}$ satisfying

$$\begin{array}{ll} \dfrac{\partial u}{\partial t} - \det \mathbf{D}^2 u = -f & \text{in } \Omega \times (0,T), \\ u = g & \text{on } \partial\Omega \times (0,T), \\ u(0) = u_0 & \text{in } \Omega. \end{array} \tag{2}$$

Here u_0 is a given function, and we assume in the sequel that it is convex, in order to favor the regularity of a smooth transient towards a stationary solution.

Numerical results will show that the right-hand side f may change sign, as long as the numerical solution of (2) remains convex and the operator in the parabolic Monge-Ampère equation remains coercive. Following [4], the Monge-Ampère operator can be rewritten under a divergence form, namely

$$\det \mathbf{D}^2 u = \frac{1}{2} \nabla \cdot \left(\mathrm{cof}(\mathbf{D}^2 u) \nabla u \right), \tag{3}$$

meaning that (2) can be interpreted as a, strongly nonlinear, parabolic equation reminiscent of a nonlinear heat equation.

When looking for a convex solution, if $\mathrm{cof}(\mathbf{D}^2 u)$ remains positive definite, then the operator is well-posed. The challenge becomes thus to capture convex solutions, and to derive numerical methods that take into account accurately the strongly nonlinear diffusion and guarantee the coercivity of the diffusion operator at all times.

2 TIME-STEPPING ALGORITHM AND SPACE DISCRETIZATION

Let $\Delta t > 0$ be a constant given time step, $t^n = n\Delta t$, $n = 1, 2, \ldots$, to define the approximations $u^n \simeq u(t^n)$. In order to handle the stiff behavior of the Monge-Ampère equation, a semi-implicit time discretization of (2) is considered. In this case, we advocate a *midpoint rule* and, u^n being known, we look for the next time step approximation u^{n+1} satisfying

$$\frac{u^{n+1} - u^n}{\Delta t} - \det \left(\mathbf{D}^2 u^{n+1/2} \right) = -f^{n+1/2} \quad n = 0, 1, \ldots, \tag{4}$$

where $u^{n+1/2} := (u^{n+1} + u^n)/2$ and $f^{n+1/2} := f\left((t^{n+1} + t^n)/2\right)$. Note that (4) is equivalent to

$$u^{n+1/2} - \Delta t \det \mathbf{D}^2 u^{n+1/2} = u^n - \frac{1}{2} \Delta t f^{n+1/2},$$

together with $u^{n+1} = 2u^{n+1/2} - u^n$. This nonlinear problem is solved with a safeguarded Newton method at each time step. Details can be found in [2].

For the space discretization, let us denote by $h > 0$ a space discretization step, together with an associated *triangulation* $\mathcal{T}_h$ of Ω. We associate with $\mathcal{T}_h$ a finite element method based on continuous piecewise linear finite elements. We denote by u_h^n the piecewise linear continuous approximation of the solution u at time t^n, and by u_h the approximation of the stationary solution. The approximation of the second derivatives is achieved via a mixed method with regularization, as mentioned below.

3 ADAPTIVE ALGORITHM

We'd like to consider the Monge-Ampère equation in presence of singularities. These non-smooth examples include cases with an exact solution with less or no regularity, or cases without an exact classical solution. A mesh adaptive strategy is thus advocated in order to increase the accuracy of the approximation of the solution. The adaptive algorithm in incorporated into the time-stepping approach, at given time steps, to capture the stationary solution. Our goal is to build an adaptive mesh such that the estimated relative error is close to a given tolerance TOL, namely:

$$0.5\ TOL \leq \frac{\eta}{||\nabla u_h||_{L^2(\Omega)}} \leq 1.5\ TOL,$$

where the (isotropic) error indicator η is computed from a finite element approximation, and u_h is the finite element approximation of the stationary solution u of (1) [2]. With (1) and (3), the stationary problem reads as follows: find $u : \Omega \to \mathbb{R}$ such that

$$\begin{cases} \frac{1}{2}\nabla \cdot \big(\mathrm{cof}(\mathbf{D}^2 u)\nabla u\big) = f & \text{in } \Omega, \\ u = g & \text{on } \partial\Omega, \end{cases} \tag{5}$$

Let us define $V_g = \{w \in H^1(\Omega) : w|_{\partial\Omega} = g\}$. The weak formulation of (5) corresponds to: find $u \in V_g$ such that:

$$\frac{1}{2}\int_\Omega \mathrm{cof}(\mathbf{D}^2 u)\nabla u \cdot \nabla v d\mathbf{x} = -\int_\Omega f v d\mathbf{x}, \quad \forall v \in H_0^1(\Omega). \tag{6}$$

Let us denote by $V_{g,h}$ the space of continuous piecewise linear functions over $\mathcal{T}_h$ satisfying the appropriate boundary condition g. The discrete problem reads: find $u_h \in V_{g,h}$ such that:

$$\frac{1}{2}\int_\Omega \mathrm{cof}(\mathbf{D}_h^2 u_h)\nabla u_h \cdot \nabla v_h d\mathbf{x} = -\int_\Omega f v_h d\mathbf{x}, \quad \forall v_h \in V_{0,h}.$$

The approximation $\mathbf{D}_h^2 u_h \in V_{0,h}$ is achieved via a mixed finite element method with a *Tychonoff regularization* procedure, as detailed in [1].

The error estimate that we derive is based on a classical residual approach [5]. We assume for the derivation that $g \equiv 0$. Let $R(u - u_h)$ be the residual defined, for all $v \in H_0^1(\Omega)$, by:

$$\begin{aligned}\langle R(u-u_h),v\rangle &= \frac{1}{2}\int_\Omega \left(\mathrm{cof}(\mathbf{D}^2u)\nabla u - \mathrm{cof}(\mathbf{D}_h^2u_h)\nabla u_h\right)\cdot\nabla v d\mathbf{x}\\ &= -\int_\Omega f v d\mathbf{x} - \frac{1}{2}\int_\Omega \mathrm{cof}(\mathbf{D}_h^2u_h)\nabla u_h\cdot\nabla v d\mathbf{x}.\end{aligned}$$

Proceeding as in [5], we obtain

$$\langle R(u-u_h),v\rangle \leq c\left(\sum_{K\in\mathcal{T}_h}(\eta_K)^2\right)^{\frac{1}{2}}||\nabla v||_{L^2(\Omega)}. \tag{7}$$

where c is a constant that depends on the mesh aspect ratio, but that is independent of the data f and mesh size h, and where

$$\begin{aligned}(\eta_K)^2 &= h_K^2||-f+\frac{1}{2}\nabla\cdot\left(\mathrm{cof}(\mathbf{D}_h^2u_h)\nabla u_h\right)||^2_{L^2(K)} + \frac{1}{16}h_K||\left[\mathrm{cof}(\mathbf{D}_h^2u_h)\nabla u_h\cdot\mathbf{n}\right]||^2_{L^2(\partial K)}\\ &= h_K^2||-f+\det\mathbf{D}_h^2u_h||^2_{L^2(K)} + \frac{1}{16}h_K||\left[\mathrm{cof}(\mathbf{D}_h^2u_h)\nabla u_h\cdot\mathbf{n}\right]||^2_{L^2(\partial K)},\end{aligned}$$

and $[\cdot]$ denotes the jump of the inside quantity on the internal edges. The error indicator η is thus defined by $\eta=\left(\sum_{K\in\mathcal{T}_h}(\eta_K)^2\right)^{\frac{1}{2}}$. Using (6), we also obtain:

$$\begin{aligned}\langle R(u-u_h),u-u_h\rangle &= \frac{1}{2}\int_\Omega\left(\mathrm{cof}(\mathbf{D}^2u)\nabla u-\mathrm{cof}(\mathbf{D}_h^2u_h)\nabla u_h\right)\cdot\nabla\left(u-u_h\right)d\mathbf{x}\\ &= \frac{1}{2}\int_\Omega \mathrm{cof}(\mathbf{D}^2u)\nabla\left(u-u_h\right)\cdot\nabla\left(u-u_h\right)\\ &\quad+\frac{1}{2}\int_\Omega\left(\mathrm{cof}(\mathbf{D}^2u)-\mathrm{cof}(\mathbf{D}_h^2u_h)\right)\nabla u_h\cdot\nabla\left(u-u_h\right)d\mathbf{x}.\end{aligned}$$

Assuming that u is strictly convex we obtain

$$\begin{aligned}\langle R(u-u_h),u-u_h\rangle \geq\ & \frac{\lambda_1}{2}||\nabla\left(u-u_h\right)||^2_{L^2(\Omega)}\\ & -\frac{1}{2}||\left(\mathrm{cof}(\mathbf{D}^2u)-\mathrm{cof}(\mathbf{D}_h^2u_h)\right)\nabla u_h||_{L^2(\Omega)}\,||\nabla\left(u-u_h\right)||_{L^2(\Omega)},\end{aligned} \tag{8}$$

where λ_1 is the smallest eigenvalue of $\mathrm{cof}(\mathbf{D}^2u)$. Finally (7) and (8) lead to:

$$\frac{\lambda_1}{2}||\nabla\left(u-u_h\right)||_{L^2(\Omega)} \leq c\,\eta+\gamma, \tag{9}$$

where the additional term $\gamma := \frac{1}{2}|| \left(\text{cof}(\mathbf{D}^2 u) - \text{cof}(\mathbf{D}_h^2 u_h)\right) \nabla u_h||_{L^2(\Omega)}$ highlights the full nonlinearity of the Monge-Ampère operator. Numerical results will show that the convergence behavior of this indicator is appropriate albeit not always optimal, as expected.

The general approach we propose to solve the elliptic Monge-Ampère equation (1) is to implement the adaptive algorithm within the time-stepping algorithm to approximate the solution of the stationary problem. The frequency of the adaptive mesh refinement is detailed in the numerical experiments.

4 NUMERICAL EXPERIMENTS

In this section, we present various test cases in order to examine the efficiency of the indicator η. For all test cases, the computational domain is the unit square $\Omega = (0,1)^2$. The initial time step is $\Delta t = 5 \times 10^{-4}$, and will be adapted depending on the number of iterations of the Newton method at each time step, see [3]. Unless specified otherwise, we initially consider a structured (asymmetric) mesh of size $h_K = 1/20$, then we perform the first mesh refinement when $||u_h^{n+1} - u_h^n||_{L_2(\Omega)} \leq 5 \times 10^{-4}$. This condition is usually reached in less than 100 timesteps. Then, we adapt the mesh every 50 timesteps, or if the same previous condition is satisfied, with a maximum of 800 timesteps. In the sequel, we define $h_{min} := \min_{K \in \mathcal{T}_h} h_K$ and $h_{max} := \max_{K \in \mathcal{T}_h} h_K$, and we enforce the condition $(h_{max}/h_{min}) \leq 40$ to avoid an unbounded number of iterations of the algorithm.

4.1 Smooth example without mesh refinement

Let us consider first a smooth exponential example:

$$\begin{cases} \det \mathbf{D}^2 u(x,y) = (x+y+1)\, e^{\left(x^2+y^2\right)} & \forall (x,y) \in \Omega, \\ u(x,y) = e^{\frac{1}{2}\left(x^2+y^2\right)} & \forall (x,y) \in \partial\Omega. \end{cases}$$

The convex solution u of this problem is $u(x,y) = e^{\frac{1}{2}\left(x^2+y^2\right)}$ for all $(x,y) \in \Omega$. In this example we use a triangular unstructured mesh and we vary h_K uniformly, with a stopping criterion given by $||u_h^{n+1} - u_h^n||_{L_2(\Omega)} \leq 10^{-7}$. Without adapting the mesh, the objective of this example is to highlight the appropriate properties of the error indicator η on smooth solutions and unstructured refined mesh. Table 1 shows that the H^2 error norm, the estimation of γ, and the error indicator η converge with order $O(h)$. Note that the additional factor γ is not negligible but converges with same order as the error indicator; however, as emphasized in [1], we can expect a better convergence behavior when the mesh is a structured one.

4.2 Non-smooth example

Let us consider a non-smooth problem:

Table 1: Smooth exponential example with uniformly refined mesh. Estimated errors of $u - u_h$, values of the indicator η, number of time steps, and the corresponding convergence orders for various h_K.

h_K	η	rate	$\frac{\eta}{\lvert u-u_h\rvert_{H^1(\Omega)}}$	$\lvert\lvert\mathbf{D}^2u-\mathbf{D}_h^2u_h\rvert\rvert_{L^2(\Omega)}$	rate	γ	rate	Timesteps
0.03125	6.29e-01	-	8.51	7.17e-01	-	4.81e-01	-	150
0.01561	3.33e-01	0.91	11.40	4.74e-01	0.59	3.42e-01	0.49	247
0.01035	2.18e-01	1.04	12.72	3.06e-01	1.07	2.26e-01	1.02	378
0.00776	1.63e-01	1.01	13.60	2.30e-01	0.99	1.69e-01	1.01	379

$$\begin{cases} \det \mathbf{D}^2u(x,y) = \dfrac{R^2}{\left(R^2-(x-0.5)^2-(y-0.5)^2\right)^2} & \forall (x,y)\in\Omega, \\ u(x,y) = -\sqrt{R^2-(x-0.5)^2-(y-0.5)^2} & \forall (x,y)\in\partial\Omega, \end{cases} \tag{10}$$

where $R = 1/\sqrt{2}$. The exact solution u of problem (10) is given by

$$u(x,y) = -\sqrt{R^2-(x-0.5)^2-(y-0.5)^2}, \quad \forall (x,y)\in\bar{\Omega}.$$

Note that the solution u is smooth in $\overline{\Omega}$ but ∇u is discontinuous in the four corners of $\overline{\Omega}$. Figure 1 illustrates the refined meshes for various TOL, and shows an appropriate tracking of the discontinuities by mesh refinement in the corners of the domain. Numerical results are illustrated in Table 2; when TOL decreases, h_{min}, h_{max} and the L^2 error norm decrease while the number of elements and nodes increase for both solvers. However, the indicator η and the H^1 error norm do not decrease for decreasing TOL. This test case being out of the classical theoretical framework, this behavior is probably due to the singularity of the gradient of the solution.

Table 2: Non-smooth example with data $f(x,y) = \frac{R^2}{(R^2-(x-0.5)^2-(y-0.5)^2)^2}$, $g(x,y) = -\sqrt{R^2-(x-0.5)^2-(y-0.5)^2}$ and $R = \frac{1}{\sqrt{2}}$. Convergence behavior of the algorithm for various values of parameter TOL (final minimal and maximal mesh size, final numbers of elements and nodes, value of the indicator, H^1 and L^2 error norms). Results obtained after 800 timesteps.

TOL	h_{min}	h_{max}	# elem	# nodes	η	$\lvert\mathbf{u}-\mathbf{u}_h\rvert_{H^1}$	$\lvert\lvert\mathbf{u}-\mathbf{u}_h\rvert\rvert_{L^2}$
1.0	6.65e-03	1.43e-01	916	523	0.36e+01	1.32e-01	4.41e-03
0.5	3.00e-03	9.60e-02	2949	1612	0.65e+01	9.30e-02	1.23e-03
0.25	2.03e-03	5.57e-02	9217	4889	1.18e+01	1.03e-01	5.75e-04

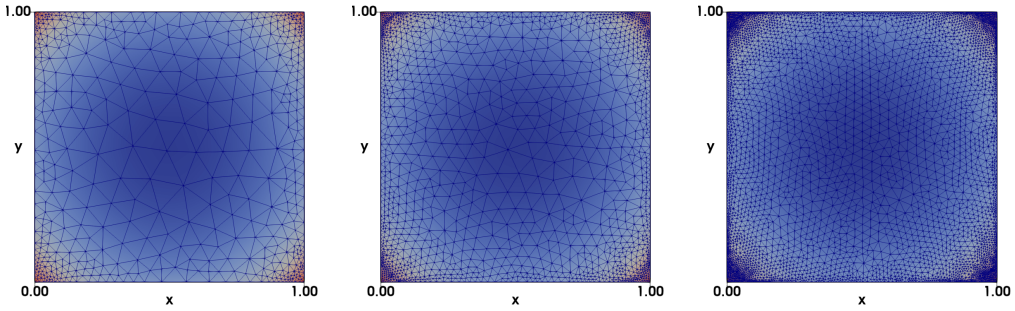

TOL = 1.0 TOL = 0.5 TOL = 0.25

Figure 1: Non-smooth example with data $f(x,y) = \frac{R^2}{(R^2-(x-0.5)^2-(y-0.5)^2)^2}$, $g(x,y) = -\sqrt{R^2-(x-0.5)^2-(y-0.5)^2}$ and $R = \frac{1}{\sqrt{2}}$. Graphs of the final adapted mesh for various values of TOL obtained after 800 timesteps.

4.3 Example without an exact solution

Another non-smooth problem that we consider is

$$\begin{cases} \det \mathbf{D}^2 u(x,y) = 1 & \forall (x,y) \in \Omega, \\ u(x,y) = 0 & \forall (x,y) \in \partial\Omega, \end{cases} \tag{11}$$

Despite the smooth data, this problem does not admit a classical solution. As mentioned in [1], the main difficulties occur nearby the boundary of the domain. This is confirmed in Figure 2, where the refined meshes are displayed for different TOL. For $TOL \leq 0.5$, the algorithm successfully refines the mesh around the boundary and keeps a coarser mesh in the center of the domain. Table 3 shows in particular that the indicator η does not decrease for decreasing TOL. We note that, when $TOL = 0.25$, the reason why the minimal mesh size h_{min} does not decrease remains to be investigated.

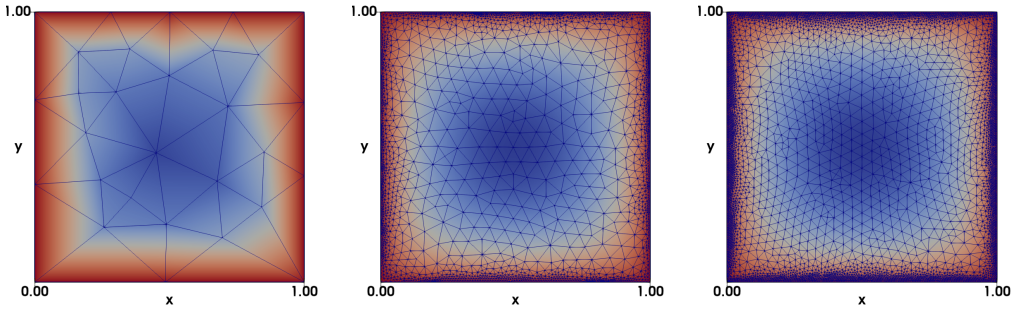

TOL = 1.0 TOL = 0.5 TOL = 0.25

Figure 2: Non-smooth example with data $f(x,y) = 1$ and $g(x,y) = 0$. Graphs of the final adapted mesh for various values of TOL obtained after 800 timesteps.

Table 3: Non-smooth example with data $f(x,y) = 1$ and $g(x,y) = 0$. Convergence behavior of the algorithm for various values of parameter TOL (final minimal and maximal mesh size, final numbers of elements and nodes, value of the indicator, and minimal solution of u_h error norm). Results obtained after 800 timesteps.

TOL	h_{min}	h_{max}	# elem	# nodes	η	$\min(u_h)$
1.0	1.31e-01	3.16e-01	46	30	4.41e-01	-0.168726
0.5	2.89e-03	8.61e-02	4454	2496	2.82e-01	-0.173368
0.25	2.76e-03	5.40e-02	9916	5279	5.83e-01	-0.179461

5 CONCLUSIONS

We have derived an isotropic error estimate to introduce an adaptive mesh refinement method for the solution of the elliptic Monge-Ampère equation. The adaptive algorithm is inserted into a time-stepping scheme for an evolutive Monge-Ampère equation. It allows to track more accurately the singularities of the solution or of its gradient. Numerical experiments have exhibited optimal convergence properties for smooth cases, but to be improved when in presence of singularities.

REFERENCES

[1] A. Caboussat, R. Glowinski, and D. C. Sorensen. A least-squares method for the numerical solution of the Dirichlet problem for the elliptic Monge-Ampère equation in dimension two. *ESAIM: Control, Optimization and Calculus of Variations*, 19(3):780–810, 2013.

[2] A. Caboussat and D. Gourzoulidis. A second order time stepping method for the approximation of a parabolic 2D Monge-Ampère equation. In *Proceedings of Numerical Mathematics and Advanced Applications ENUMATH 2019*, volume 139. Springer, 2021.

[3] D. Gourzoulidis. *Numerical Methods for First and Second Order Fully Nonlinear Partial Differential Equations*. PhD thesis, Ecole Polytechnique Fédérale de Lausanne, 2021.

[4] H. Liu, R. Glowinski, S. Leung, and J. Qian. A finite element/operator-splitting method for the numerical solution of the three dimensional Monge-Ampère equation. *Journal of Scientific Computing*, 81(3):2271–2302, 2019.

[5] R. Verfürth. *A review of a posteriori error estimation and adaptive mesh-refinement techniques*, page 1–127. Advances in numerical mathematics. Wiley, 1996.